

# On the phenomenological analyses of $s$ - $\bar{s}$ asymmetry in the nucleon sea

Fu-Guang Cao\* and A. I. Signal†

*Institute of Fundamental Sciences, Massey University, Private Bag 11 222, Palmerston North, New Zealand*

Two phenomenological models which give opposite predictions for the  $s$ - $\bar{s}$  asymmetry in the nucleon sea are re-analyzed carefully. It is pointed out that although the quantitative results in both models depend dramatically on the parameters, the predictions for the shape of  $s(x) - \bar{s}(x)$  in the two models are parameter independent and opposite. Thereby the coming experiments are likely to be able to distinguish the two models. We find that the reason for the two models giving opposite predictions is that the fluctuation functions and parametrizations for the strange (anti-strange) quark distribution in the baryon (meson) in the two models are quite different. To further investigate these models, we use the same parametrizations for the strange (anti-strange) distributions of the baryon (meson) in the two models. We find that one of the models depends strongly on the parameter which controls the behavior of the meson-baryon fluctuation function. Also the two models agree on the shape and size of  $s$ - $\bar{s}$  for some values of the model parameters, but can disagree strongly for others.

PACS number(s): 13.60.Hb; 11.30.Hv; 12.39.Ki; 13.88.+e

---

\*E-mail address: f.g.cao@massey.ac.nz.

†E-mail address: a.i.signal@massey.ac.nz.

## I. INTRODUCTION

Studying the light quark content in the nucleon sea is important to the understanding of nucleon structure as well as strong interaction. There is strong experimental evidence that the light quark sea is flavor asymmetric i.e.  $\bar{u} \neq \bar{d}$  [1–4]. Another interesting question concerning the dynamics of the light quark sea of the nucleon is quark-antiquark ( $q$ - $\bar{q}$ ) asymmetry. The nucleon sea can be broken down into perturbative (“extrinsic”) and non-perturbative (“intrinsic”) parts. The perturbative sea is created from gluon-splitting and can be calculated from perturbative QCD as the  $q\bar{q}$  pair exists only for short times. In the leading twist approximation, the perturbative sea is symmetric, i.e.  $q = \bar{q}$ . The non-perturbative sea, however, may exist over a long time and it has a strong connection with the “bare” nucleon. There is no fundamental theoretical principle and/or experimental evidence which demands that the non-perturbative sea is symmetric. Although it is usually assumed that the quark sea in the nucleon is equal to the anti-quark sea, one should note that the  $q$ - $\bar{q}$  symmetry may be violated to some extent. Because one can not distinguish the sea up and down quarks from the valance up and down quarks in the nucleon bound state, it is difficult to study the  $q$ - $\bar{q}$  asymmetry of the up quark sea and the down quark sea in experiments. However, the strange content of the nucleon sea is accessible to experiments [5–7]. Although there is still large uncertainty in the extraction of  $s$  and  $\bar{s}$  distributions from experimental data [5–7], the analysis of [7] strongly suggests that  $s(x) \neq \bar{s}(x)$ . We can expect that the experimental data will be improved in the near future.

There have also been some theoretical analyses on this issue [8–12]. From the chiral Gross-Neveu model, Burckhardt and Warr [8] suggested that a large  $s$ - $\bar{s}$  asymmetry may exist in the nucleon sea. Due to its success in the study of the flavor asymmetry of the nucleon sea, the meson cloud model (MCM) has also been used in the study of the strange sea of the nucleon. Employing the meson cloud model with the fluctuation function calculated from covariant perturbative theory and cloudy bag model [13] Signal and Thomas [9] predicted that the  $s$  and  $\bar{s}$  can have quite different shapes, although the quantitative results depended on the bag radius. Holtmann, Szczerba and Speth [10] performed their analysis using the meson cloud model with the fluctuation function being calculated from time-order perturbative theory in the infinite momentum frame and the parameter in the form factor being fixed by the high-energy particle production data. It was found that  $s < \bar{s}$  in small  $x$  region and  $s > \bar{s}$  in large  $x$  region. Brodsky and Ma [11] proposed a light-cone two-body wave function model (LCM) for the description of the meson-baryon fluctuation, and they obtained a significantly different conclusion from [10]:  $s > \bar{s}$  ( $s < \bar{s}$ ) in the small (large)  $x$  region. The quantitative predictions in [11] dramatically depend on the normalization of the fluctuation. More recently, Christiansen and Magnin [12] arrived a similar conclusion as [11] by employing both effective and perturbative degrees of freedom and incorporating the recombination mechanism which has been well used in the study of the hadron production. It is worth to note that the same physical picture – nucleon fluctuating to meson and baryon, has been used in both MCM [9,10] and LCM [11], but the predictions for the  $s(x) - \bar{s}(x)$  are quite different.

The purpose of this paper is to re-analyze the  $s$ - $\bar{s}$  asymmetry of the nucleon sea in the frameworks of both the MCM [9,10] and LCM [11], and to find the reason that quite different predictions are obtained from the two models in which the same physical picture is employed. In sections II and III, we analyze the meson cloud model and light-cone model respectively.

In section IV, we investigate the model-dependence of the two models and present more discussions. The last section is reserved for a summary.

## II. MESON CLOUD MODEL

The meson cloud model was first suggested and developed in the studies of low energy physics and it has been proved to be a successful tools in understanding both nucleon structure and dynamics. Lately, this model has been applied to the studies of structure function and sea content of nucleon [14,15]. The basic idea of the meson cloud model is that the nucleon can be viewed as a bare nucleon surrounded by a mesonic cloud. The nucleon wave function is expressed in terms of a series of baryon and meson components. For the strange content of the nucleon sea, the important components are  $\Lambda K$  and  $\Sigma K$  Fock states,

$$\begin{aligned} |N\rangle_{\text{physical}} = & |N\rangle_{\text{bare}} + \sum_{\lambda\lambda'} \int dy d^2\mathbf{k}_\perp \phi_{\Lambda K}^{\lambda\lambda'}(y, k_\perp^2) |\Lambda^\lambda(y, \mathbf{k}_\perp); K^{\lambda'}(1-y, -\mathbf{k}_\perp)\rangle \\ & + \sum_{\lambda\lambda'} \int dy d^2\mathbf{k}_\perp \phi_{\Sigma K}^{\lambda\lambda'}(y, k_\perp^2) |\Sigma^\lambda(y, \mathbf{k}_\perp); K^{\lambda'}(1-y, -\mathbf{k}_\perp)\rangle \\ & + \dots, \end{aligned} \quad (1)$$

where  $\phi_{\Lambda K(\Sigma K)}^{\lambda\lambda'}(y, k_\perp^2)$  is the wave function of the Fock state containing a  $\Lambda$  ( $\Sigma$ ) baryon with longitudinal momentum fraction  $y$ , transverse momentum  $\mathbf{k}_\perp$ , and helicity  $\lambda$ , and a  $K$  meson with momentum fraction  $1-y$ , transverse momentum  $-\mathbf{k}_\perp$ , and helicity  $\lambda'$ . The model assumes that the lifetime of a virtual baryon-meson Fock state is much larger than the interaction time between the hard photon and nucleon in deep inelastic scattering, thus the non-perturbative contributions to the strange and anti-strange distributions in the proton,  $s^N$  and  $\bar{s}^N$ , can be written as convolutions

$$s^N(x) = \int_x^1 \frac{dy}{y} f_{BK}(y) s^B\left(\frac{x}{y}\right), \quad (2)$$

$$\bar{s}^N(x) = \int_x^1 \frac{dy}{y} f_{KB}(y) \bar{s}^K\left(\frac{x}{y}\right), \quad (3)$$

where  $B = \Lambda$  ( $\Sigma$ ),  $s^B$  and  $\bar{s}^K$  are the  $s$  and  $\bar{s}$  distributions in the  $\Lambda$  ( $\Sigma$ ) and  $K^+$  respectively, and  $f_{BK}$  is fluctuation function which describes the possibility for a nucleon fluctuating into a  $\Lambda K$  ( $\Sigma K$ ) state,

$$f_{BK}(y) = \sum_{\lambda\lambda'} \int_0^\infty dk_\perp^2 \left| \phi_{BK}^{\lambda\lambda'}(y, k_\perp^2) \right|^2. \quad (4)$$

From Eqs. (2) and (3) we know that  $s$  and  $\bar{s}$  distributions in the nucleon are different and the difference  $s - \bar{s}$  depends on both the fluctuation functions ( $f_{BK}$  and  $f_{KB}$ ) and valance quark distributions in the baryon and meson ( $s^B$  and  $\bar{s}^K$ ). Due to the baryons  $\Lambda$  and  $\Sigma$  being heavier than the  $K$  meson, the  $f_{BK}(y)$  peaks at  $y > 0.5$  while the  $f_{KB}(y)$  peaks at  $y < 0.5$  (see Fig. 5), which suggests that  $s^N > \bar{s}^N$  in the large  $x$  region. On the other hand, in the large  $x$  region the  $\bar{s}$  distribution of the  $K$  meson ( $\bar{s}^K(x)$ ) is generally believed to be larger than the  $s$  distribution of the baryon ( $s^B(x)$ ) as the baryon contains one more valance

quark than the meson (see Fig. 4). This implies that  $s^N < \bar{s}^N$  in the large  $x$  region. The final prediction of the  $x$  dependence of  $s$ - $\bar{s}$  asymmetry will depend on these two competing effects.

From the consideration of momentum and charge conservation, we have

$$f_{BK}(y) = f_{KB}(1 - y). \quad (5)$$

It has been pointed out [10,16,17] that the constraint Eq. (5) can be guaranteed in the calculation employing time-ordered perturbative theory (TOPT) in the infinite momentum frame while it cannot be satisfied automatically in the covariant perturbation calculation. Another advantage of employing the TOPT in the infinite momentum frame is that the intermediate particles (baryons and mesons) are on their mass-shell and so there is no ambiguity associated with the possible off-mass-shell behavior of their structure functions which are encountered in the covariant perturbative formulations.

The wave function  $\phi_{BK}^{\lambda\lambda'}$  in Eq. (4), and thereby the fluctuation function  $f_{BK}(y)$ , can be calculated from the effective meson-baryon-nucleon interaction Lagrangian,

$$L = g \cdot i\bar{\psi}\gamma_5\phi\psi, \quad (6)$$

where  $g$  is the effective coupling constant, and  $\psi$  and  $\phi$  are the nucleon and pseudoscalar fields respectively. Employing time-ordered perturbative theory in the infinite momentum frame, we obtain

$$f_{BK}^{\text{MCM}}(y) = \frac{g_{NBK}^2}{16\pi^2} \int_0^\infty \frac{dk_\perp^2}{y(1-y)} \frac{G_{BK}^2(y, k_\perp^2)}{(m_N^2 - m_{BK}^2)^2} \frac{(ym_N - m_B)^2 + k_\perp^2}{y}, \quad (7)$$

where  $m_{BK}^2$  is the invariant mass squared of the  $\Lambda K$  ( $\Sigma K$ ) Fock state,

$$m_{BK}^2 = \frac{m_B^2 + k_\perp^2}{y} + \frac{m_K^2 + k_\perp^2}{1-y}, \quad (8)$$

and  $G_{BK}(y, k_\perp^2)$  is a phenomenological vertex form factor for which we adopt a exponential form [10]

$$G_{BK}(y, k_\perp^2) = \exp \left[ \frac{m_N^2 - m_{BK}^2(y, k_\perp^2)}{2\Lambda^2} \right]. \quad (9)$$

It has been argued in Ref. [10] from studies of baryon production processes that a unique cut-off parameter  $\Lambda = 1.08$  GeV can be used for all vertices involving octet baryons and pseudoscalar or vector mesons. The fluctuation functions for the different charge states can be obtained by using the following relations:

$$f_{\Lambda K^+}(y) = f_{\Lambda K}(y), \quad (10)$$

$$f_{\Sigma^+ K^0}(y) = 2 f_{\Sigma^0 K^+}(y) = 2 f_{\Sigma K}(y), \quad (11)$$

where  $f_{\Lambda K}(y)$  and  $f_{\Sigma K}(y)$  are given by Eq. (7) with  $B$  being  $\Lambda$  and  $\Sigma$  respectively. We take the effective coupling constants  $g_{N\Lambda K}^2/4\pi = 13.7$  and  $g_{N\Sigma K}^2/4\pi = 3.7$  [9,18].

For the  $s$  distribution in the  $\Lambda$  ( $\Sigma$ ) it is common practice to use the parametrization for the valance quark distribution in the nucleon via relation [9,10,12]

$$s^B = \frac{u^N}{2}. \quad (12)$$

Here, we adopt the next-leading-order parametrization given in [19] (GRV98) for  $u^N$  at scale  $\mu_{NLO}^2 = 0.40$  GeV $^2$ ,

$$u^N(x, \mu_{NLO}^2) = 0.632x^{-0.57}(1-x)^{3.09}(1+18.2x). \quad (13)$$

For the  $\bar{s}$  distribution in the  $K$ , we adopt the parametrization of [20] (GRS98) which is obtained by connecting  $\bar{s}^K$  with the valance quark distribution in the pionic meson based on the consistent quark model,

$$\bar{s}^{K^+}(x, \mu_{NLO}^2) = v^\pi(x, \mu_{NLO}^2) - u^{K^+}(x, \mu_{NLO}^2), \quad (14)$$

with

$$v^\pi(x, \mu_{NLO}^2) = 1.052x^{-0.495}(1+0.357\sqrt{x})(1-x)^{0.365}, \quad (15)$$

$$u^{K^+}(x, \mu_{NLO}^2) = 0.540(1-x)^{0.17}v^\pi(x, \mu_{NLO}^2), \quad (16)$$

at scale  $\mu_{NLO}^2 = 0.34$  GeV $^2$ . The numerical result is given in Fig. 1. It can be found that  $s^N > \bar{s}^N$  as  $0.02 < x < 0.21$  and  $s^N < \bar{s}^N$  as  $x > 0.21$ .

### III. LIGHT-CONE MODEL

As is well known, the nucleon is built up from three valance quarks plus  $q\bar{q}$  pairs and gluons which compose the nucleon sea. The light-cone (LC) formalism [21] provides a convenient framework for the relativistic description of hadrons in terms of quark and gluon degrees of freedom. Combined with perturbation theory, the light-cone formalism has been applied to many exclusive processes with large momentum transfer. In this formalism, the quantization is chosen at a particular light-cone time  $\tau = t+z$ . The hadronic wave function, which describes the hadronic composite state at a particular  $\tau$ , can be expressed in terms of a series of light-cone wave functions multiplied by the Fock states. For example,

$$|p\rangle = |uud\rangle \psi_{uud/p} + |uudg\rangle \psi_{uudg/p} + \sum_{q\bar{q}} |uudq\bar{q}\rangle \psi_{uudq\bar{q}/p} + \dots \quad (17)$$

As an approximation, Brodsky and Ma [11] suggested that the nucleon wave function Eq. (17) could also be expressed as a sum of baryon-meson Fock states similar to Eq. (1). In principle, the predictions obtained by employing effective degrees of freedom [Eq. (1)] should coincide with the results from employing the quark-gluon degrees of freedom [Eq. (17)]. The probability of the baryon-meson fluctuation should decrease with the invariant mass of the baryon-meson Fock state increasing. So the  $\Lambda K$  and  $\Sigma K$  Fock states are the most important states in the study of the strange sea of nucleon, whereas the higher Fock states will be less important. It was pointed out in Ref. [11] that the possibility for finding the  $\Lambda K^{*+}$  state is only about 5%  $\sim$  10% of the possibility for finding the  $\Lambda K^+$  state.

In the light-cone baryon-meson fluctuation model, the same two-level convolution mechanism and formula (see Eqs. (2), (3), (5) and discussion following them) are employed to evaluate the non-perturbative contribution to the  $s$  and  $\bar{s}$  content in the proton sea. However,

the two factors inside the convolution integrals, the fluctuation function ( $f_{BK}$  and  $f_{KB}$ ) and valance quark distributions in the baryon and meson ( $s^B$  and  $\bar{s}^K$ ), are now both described using two-body light-cone wave functions. The probability of the baryon-meson fluctuation (the fluctuation function) is given by

$$f_{BM}^{\text{LCM}}(y) = \int_0^\infty \frac{d\mathbf{k}_\perp^2}{16\pi^2} |\psi(y, \mathbf{k}_\perp)|^2, \quad (18)$$

where  $\psi(y, \mathbf{k}_\perp)$  is a two-body wave function which is a function of the invariant mass square of the baryon-meson state [see Eq. (8)]. In Ref. [11], two wave function models, Gaussian type and power-law type, were used, but nearly identical predictions for the strange content of the nucleon sea were obtained. Hence in our calculations, we adopt the Gaussian type wave function,

$$\psi(y, \mathbf{k}_\perp) = A \exp \left[ \frac{1}{8\alpha^2} \left( \frac{m_B^2 + \mathbf{k}_\perp^2}{y} + \frac{m_K^2 + \mathbf{k}_\perp^2}{1-y} \right) \right], \quad (19)$$

where  $\alpha$  is a phenomenological parameter which determines the shape of the fluctuation function and  $\alpha = 0.33$  GeV is taken in Ref. [11]. We will discuss the  $\alpha$ -dependence of the LCM in the next section. Here we would like to point out that the constraint for the fluctuation functions,  $f_{BK}(y) = f_{KB}(1-y)$ , is satisfied automatically in the LCM [see Eqs. (18) and (19)]. For simplicity, the fluctuation function  $f_{BM}^{\text{LCM}}(y)$  was normalized to 1 in Ref. [11], thus only strikingly different  $s$  and  $\bar{s}$  distributions were observed but no absolute magnitude was given. In order to make a meaningful comparison with the result of MCM, we require that  $f_{BK}^{\text{LCM}}$  has the same normalization as  $f_{BK}^{\text{MCM}}$  with  $\Lambda = 1.08$  GeV, that is the probabilities of finding the  $\Lambda K^+$  and  $\Sigma^0 K^+$  Fock states in the nucleon are  $P_{\Lambda K^+} = 1.27\%$  and  $P_{\Sigma^0 K^+} = 0.25\%$  respectively<sup>3</sup>. Furthermore, in Ref. [11] the  $s$  distribution in the  $\Lambda$  and the  $\bar{s}$  distribution in the  $K$  are also estimated by using a Gaussian type two body wave function with the  $ud$  pair in the  $\Lambda$  being treated as a spectator,

$$s^B(x) = \int \frac{d\mathbf{k}_\perp^2}{16\pi^2} \left| A \exp \left[ \frac{1}{8\alpha^2} \left( \frac{m_s + \mathbf{k}_\perp^2}{x} + \frac{m_D + \mathbf{k}_\perp^2}{1-x} \right) \right] \right|^2, \quad (20)$$

$$\bar{s}^K(x) = \int \frac{d\mathbf{k}_\perp^2}{16\pi^2} \left| A \exp \left[ \frac{1}{8\alpha^2} \left( \frac{m_s + \mathbf{k}_\perp^2}{x} + \frac{m_q + \mathbf{k}_\perp^2}{1-x} \right) \right] \right|^2. \quad (21)$$

The mass parameters are taken as  $m_q = 330$  MeV for the light-flavor quark,  $m_s = 480$  MeV for the  $s$  quark, and  $m_D = 600$  MeV for the spectator [11]. The strange and anti-strange distributions in the nucleon sea are obtained via Eqs. (2) and (3). The numerical result is given in Fig. 1. One can find that  $s^N < \bar{s}^N$  as  $0.02 < x < 0.24$  and  $s^N > \bar{s}^N$  as  $x > 0.24$ , which is opposite to the predictions from the MCM.

#### IV. MODEL-DEPENDENCE AND DISCUSSIONS

The predictions from the two phenomenological models (MCM and LCM) are quite different. We want to make a comparison between the two models and clarify the difference

---

<sup>3</sup>Note from Eq. (11) the probability of finding the  $\Sigma^+ K^0$  Fock state is  $P_{\Sigma^+ K^0} = 0.50\%$ .

between them. We then hope that more precise experimental data will enable us to make a choice between the two models, or at least determine their parameters.

The important parameters are  $\Lambda$  in the MCM and  $\alpha$  in the LCM. First, we study the effect of  $\Lambda$  on the calculation by allowing a range for  $\Lambda$ ,  $1.0 \text{ GeV} < \Lambda < 1.2 \text{ GeV}$ . It should be noted that the parameter  $\Lambda$  can not be varied dramatically since, in principle, it can be obtained by fitting the high-energy baryon production data. ( $\Lambda = 1.08 \pm 0.05 \text{ GeV}$  is given in [10].) The numerical results are presented in Fig. 2. It can be found that the quantitative results depend strongly on the value of  $\Lambda$ , which is not surprising since the value of  $\Lambda$  governs the probability of nucleon fluctuating to  $\Lambda$  ( $\Sigma$ ) baryon and  $K$  meson. (For  $\Lambda = 1.00 \text{ GeV}$ ,  $1.08 \text{ GeV}$ , and  $1.20 \text{ GeV}$ ,  $P_{\Lambda K} = 0.83\%$ ,  $1.27\%$ , and  $2.42\%$ .) However, the prediction for the shape of  $s(x) - \bar{s}(x)$  in the MCM is quite independent of the value of  $\Lambda$  –  $s(x) - \bar{s}(x)$  is negative for  $0.02 < x < 0.21$  and positive for  $x > 0.21$  no matter which  $\Lambda$  is chosen. We note that our range of  $\Lambda$  corresponds to a dipole form factor with cut-off parameter in the range of  $650 - 850 \text{ MeV}$  [22], which is fairly soft, and corresponds to a bag radius about  $1 \text{ fm}$  in the cloudy bag model.

In the LCM, the shapes of the fluctuation function [see Eq. (18)] as well as the strange (anti-strange) distribution in the baryon (meson) [see Eqs. (20) and (21)] are mainly determined by the value of  $\alpha$  – they become broader as  $\alpha$  increases. The value of  $\alpha$  reflects the strength of the interaction potential in the two body bound state. Phenomenological studies show that for the pion, a value of  $\alpha$  in the range of  $300 - 500 \text{ MeV}$  is favored [23]. However, there is little constraint on the corresponding parameter  $\alpha$  when we consider the portion of the nucleon wave function arising from one baryon and one meson Fock state, since effective degrees of freedom are involved and there are few studies employing this model. In principle, the parameters  $\alpha$  and  $A$  involved in Eq. (19) can be fixed by fitting high-energy baryon and meson production data and experimental information on the  $\bar{d}\bar{u}$  asymmetry in the proton [1–4], however this is beyond the scope of the present study and will be the subject of future work [24]. Due to the lack of information on the value of  $\alpha$ , we study the  $\alpha$  dependence of the calculation in the LCM by varying  $\alpha$  from  $0.33 \text{ GeV}$  to  $1.00 \text{ GeV}$  (see Fig. 3). It can be found that the quantitative results strongly depend on the value of  $\alpha$ , but the prediction for the shape of  $s(x) - \bar{s}(x)$  stays the same and is opposite to the prediction of MCM –  $s(x) - \bar{s}(x)$  is positive for  $0.02 < x < 0.24$  and negative for  $x > 0.24$ . Fig. 3 is obtained by setting the probabilities of nucleon fluctuating to  $\Lambda K^+$  and  $\Sigma^0 K^+$  Fock states to be  $P_{\Lambda K^+} = 1.27\%$  and  $P_{\Sigma^0 K^+} = 0.25\%$  respectively which corresponds to taking  $\Lambda = 1.08 \text{ GeV}$  in the MCM. Changing the probabilities  $P_{\Lambda K}$  and  $P_{\Sigma K}$  will change the prediction for  $s(x) - \bar{s}(x)$  in magnitude, but the predictions for the shape of  $s(x) - \bar{s}(x)$  will persist. Thus, we conclude that although the quantitative results in both models depend on the parameters strongly, the predictions for the shape of  $s(x) - \bar{s}(x)$  in both models are parameter independent. It should be not difficult for the coming experimental data to examine these two models since significantly different predictions are obtained from both models.

It is interesting to note that although the same nucleon fluctuating to baryon and  $K$  meson physical picture and two level convolution formula [see Eqs. (2) and (3)] are employed in both MCM and LCM, the conclusion about the  $s\bar{s}$  asymmetry from the two models are dramatically different. We point out that both the strange and anti-strange distributions in  $\Lambda$  ( $\Sigma$ ) and  $K$ , and the fluctuation functions used in the two models, which are the two factors in the integrands of the two-level convolution formulas [see. Eqs. (2) and (3)], are quite different. We compare the strange distribution employed in the two model in Fig. 4.

It can be seen that the strange distributions used in the LCM exhibit a sharp peak in the medium  $x$  region, while the GRV98 and GRS98 parametrizations for  $s^B$  and  $\bar{s}^K$  emphasize the small- $x$  region strongly. Also the strange (anti-strange) distributions employed in the LCM depends on the parameter  $\alpha$  – they become less peaked as  $\alpha$  increasing from 0.33 GeV to 1.00 GeV. Up to now, experimental measurements and theoretical calculations from first principles on the strange and anti-strange distribution in the baryon  $\Lambda$  ( $\Sigma$ ) and meson  $K$  are lacking (but see Refs. [25,26]). The realistic strange distribution may be different from the two-body wave function prediction used in the LCM since only the lowest Fock state is considered and the full result should be the sum of all Fock states [27,28]. However, the  $s^B(x)$  and  $\bar{s}^K(x)$  obtained from the LCM being peaked at  $x < 0.5$  and  $x > 0.5$  respectively reflects the fact that the  $s$  quark in the  $\Lambda$  ( $\Sigma$ ) should carry a smaller amount of momentum than the  $ud$  ( $uu$ ) quark pair, and the  $\bar{s}$  quark in the  $K^+$  should carry a large amount of momentum than the  $u$  quark. The studies on the strange distribution in the baryon from a Nambu-Jona Lasinio model [29,30] and the anti-strange distribution in the  $K$  meson from a Monte Carlo [31] support the above observation. Thus, although it has been a common practice to employ the modified light valance distributions of the nucleon and pion for  $s^B$  and  $\bar{s}^K$  respectively here we would like to treat the strange distribution in the LCM and the MCM as two phenomenological models.

In Fig. 5, we compare the fluctuation functions employed in the two models. Although the same physical picture, nucleon fluctuating to baryon-meson Fock state, has been adopted in both the meson cloud model and the light-cone model, the suggested fluctuation functions are quite different [see Eqs. (4) and (18)]: while a rather simple two-body wave function is employed in the LCM [11], a more complex, effective Lagrangian model is used in the MCM [9,10]. As has been pointed out in Sec. III, we adopt the same normalization condition for both  $f_{BK}^{\text{MCM}}$  and  $f_{BK}^{\text{LCM}}$  in order to make the comparison meaningful. Using the same parameters given in Refs. [10] and [11], that is,  $\Lambda = 1.08$  GeV in Eq. (9) and  $\alpha = 0.33$  GeV in Eq. (19), we find that corresponding predictions for the fluctuation functions are very different (see Fig. 5):  $f_{BK}^{\text{MCM}}(y)$  has a maximum value at about  $y = 0.57$  while  $f_{BK}^{\text{LCM}}(y)$  has a maximum at about  $y = 0.67$ . In the non-relativistic limit, the ratio of the momentum fractions carried by the  $\Lambda$  and  $K$  should be about  $y/(1-y) \sim m_\Lambda/m_K \simeq 2.3$ , that is, the fluctuation function should be sharply peaked at about  $y = 0.7$ . Thus we know that the fluctuation function obtained from the two-body wave function model is consistent with the non-relativistic argument while the one obtained in the MCM is not. Changing the parameters  $\Lambda$  in Eq. (9) and  $\alpha$  in Eq. (19) do affect the shapes of the fluctuation functions. For example, decreasing  $\Lambda$  and/or increasing  $\alpha$  will decrease the difference between the two models. However, as we mention earlier, there is only a small range of variation in  $\Lambda$  allowed from the consideration of the corresponding high-energy baryon production data. ( $\Lambda = 1.08 \pm 0.05$  GeV is given in [10].) We present the results for  $1.0 \text{ GeV} < \Lambda < 1.2 \text{ GeV}$  in Fig. 6. It can be found that the shape of fluctuation function and the  $y$ -position at which the fluctuation function exhibits a maximum value is insensitive to the value of  $\Lambda$ . (The  $y_{\max}$  increases from 0.56 to 0.58 as  $\Lambda$  decreases from 1.20 GeV to 1.00 GeV.) Consequently, the MCM’s prediction for the shape of  $s - \bar{s}$  is independent of  $\Lambda$  although the quantitative result is sensitive to the value of  $\Lambda$  as it has been shown in Sec. II (see Fig. 2). We study the  $\alpha$  dependence of the fluctuation function by taking  $0.33 \text{ GeV} < \alpha < 1.00 \text{ GeV}$  at given probabilities  $P_{\Lambda K^+} = 1.27\%$  and  $P_{\Sigma^0 K^+} = 0.25\%$  which corresponds to take  $\Lambda = 1.08$  GeV in the MCM (see Fig. 5). From Fig. 5, one can find that the fluctuation function with  $\alpha = 0.33$

GeV is more peaked than the fluctuation function with  $\alpha = 1.00$  GeV and the  $y_{max}$  changes from 0.67 to 0.58 as  $\alpha$  increases from 0.33 GeV to 1.00 GeV. The lower value is close to the  $y_{max} \simeq 0.57$  of  $f_{BK}^{\text{MCM}}$  with  $\Lambda = 1.08$  GeV. Also the  $f_{BK}^{\text{LCM}}$  with  $\alpha = 1.00$  GeV has a similar symmetry as the  $f_{BK}^{\text{MCM}}$ . Thus we expect that the prediction of the LCM with  $\alpha = 1.00$  GeV will be similar to the result of the MCM if the same parametrizations for the strange (anti-strange) distributions are employed in the two models. Indeed our following numerical calculations confirm this expectation.

To make more concrete our above discussions about the fluctuation functions, we employ the same parametrizations for the strange and anti-strange distribution in the  $\Lambda$  ( $\Sigma$ ) and  $K$  i.e. Eq. (12) for the  $s^B$  and Eq. (14) for the  $\bar{s}^K$ , in the two models. The LCM in this case is denoted as modified light-cone model (MLCM). We present the numerical results for different values of  $\alpha$  and  $\Lambda = 1.08$  GeV in Fig. 7. It can be found that the prediction from the MLCM depends strongly on the value of  $\alpha$  – the calculation with  $\alpha = 0.33$  GeV is quite different from the result of MCM while the calculation with  $\alpha = 1.00$  GeV is quite similar to the result of MCM. Changing the value of  $\Lambda$ , which corresponds to changing the possibilities of finding the baryon-meson Fock state in the nucleon, will not greatly affect our above conclusion.

## V. SUMMARY

The  $s$ - $\bar{s}$  asymmetry in the nucleon sea is an important observable in the understanding of nucleon structure and the strong interaction. Some theoretical attempts have been made in this direction. Among them the meson cloud model and the light-cone model give significantly different predictions for both the shape of  $s(x) - \bar{s}(x)$  and the absolute magnitude. By reanalyzing these two models carefully, we point out that although the quantitative calculations in the two models both depend strongly on the model parameters, the predictions for the shape of  $s(x) - \bar{s}(x)$  from the two models are parameter independent and opposite. Thus it should be easy for more precise experimental data to distinguish between the two models. The reasons for the quite different predictions obtained in the two models are that the strange and anti-strange distributions in the baryon and meson, and the fluctuation functions employed in the two models are dramatically different.

To further investigate the two models, we modify the LCM by employing the same parametrizations for the strange and anti-strange quark distributions in the  $\Lambda$  ( $\Sigma$ ) baryon and  $K$  meson in the LCM as that in the MCM. It is found that the calculation in the modified light-cone model (MLCM) depends strikingly on the parameter  $\alpha$  which controls the behavior of the meson-baryon fluctuation function. Consequently, the  $s$ - $\bar{s}$  asymmetry of the nucleon sea from the MLCM can be different dramatically from that from the MCM in some parameter ranges, as well as very similar in other parameter ranges. The coming experimental data will examine these calculations, or equally, provide information on both the fluctuation function and strange distributions in the  $\Lambda$  ( $\Sigma$ ) baryon and  $K$  meson.

## ACKNOWLEDGMENTS

This work was partially supported by the Massey Postdoctoral Foundation, New Zealand.

## REFERENCES

- [1] P. Amaudraz et al., Phys. Rev. Lett. **66**, 2712 (1991); M. Arneodo et al., Phys. Rev. D **50**, R1 (1994); M. Arneodo et al., Phys. Lett. B **364**, 107 (1995).
- [2] A. Baldit et al., Phys. Lett. B **332**, 244 (1994).
- [3] E. A. Hawker et al., E866/NuSea Collaboration, Phys. Rev. Lett. **80**, 3715 (1998).
- [4] K. Ackerstaff et al., Hermes Collaboration, Phys. Rev. Lett. **81**, 5519 (1998).
- [5] C. Boros, J. T. Lonergan, and A. W. Thomas, Phys. Rev. Lett. **81**, 4075 (1998).
- [6] W. G. Seligman et al., CCFR-Collaboration, Phys. Rev. Lett. **79**, 1213 (1997); A. O. Bazarko et al., CCFR-Collaboration, Z. Phys. C **65**, 189 (1995); S. A. Rabinowitz et al., CCFR-Collaboration, Phys. Rev. Lett. **70**, 134 (1993).
- [7] M. Arneodo et al., NMC-Collaboration, Nucl. Phys. **B483**, 3 (1997).
- [8] M. Burckhardt and B. J. Warr, Phys. Rev. D **45**, 958 (1992).
- [9] A. I. Signal and A. W. Thomas, Phys. Lett. B **191**, 205 (1987).
- [10] H. Holtmann, A. Szczerba, and J. Speth, Nucl. Phys. **A569**, 631 (1996).
- [11] S. J. Brodsky and B. Q. Ma, Phys. Lett. B **381**, 317 (1996).
- [12] H. R. Christiansen and J. Magnin, Phys. Lett. B **445**, 8 (1998).
- [13] A. W. Thomas, Adv. Nucl. Phys. **13**, 1 (1984); G. A. Miller, in: Intern. Rev. Nucl. Phys., Vol. **2** (1984).
- [14] J. D. Sullivan, Phys. Rev. D **5**, 1732 (1972).
- [15] see for example, A. W. Thomas, Phys. Lett. B **126**, 97 (1983).
- [16] V. R. Zoller, Z. Phys. C **53**, 443 (1992).
- [17] W. Melnitchouk, J. Speth, and A. W. Thomas, Phys. Rev. D **59**, 014033 (1999).
- [18] J. J. Aubert et al., Phys. Lett. B **123**, 275 (1983).
- [19] M. Glück, E. Reya, and A. Vogt, Eur. Phys. J. C **5**, 461 (1998).
- [20] M. Glück, E. Reya, and M. Stratmann, Eur. Phys. J. C **2**, 159 (1998).
- [21] See, *e.g.*, J. B. Kogut and D. E. Soper, Phys. Rev. D **1**, 2901 (1970); J. B. Bjorken, J. B. Kogut, and D. E. Soper, *ibid.* **3**, 1328 (1971); S. J. Brodsky, R. Roskies, and R. Suaya, *ibid.* **8**, 4574 (1973).
- [22] W. Melnitchouk and A. W. Thomas, Phys. Rev. D **47**, 3794 (1993).
- [23] T. Huang, B. Q. Ma, and Q. X. Shen, Phys. Rev. D **49**, 1490 (1994).
- [24] F. G. Cao and A. I. Signal, in preparation.
- [25] M. Alberg, E. M. Henley, X. Ji, and A. W. Thomas, Phys. Lett. B **389**, 367 (1996).
- [26] C. Boros and A. W. Thomas, hep-ph/9902372.
- [27] S. J. Brodsky and G. P. Lepage, Phys. Rev. Lett. **43**, 545 (1979); Phys. Lett. **87B**, 359 (1979); G. P. Lepage and S. J. Brodsky, Phys. Rev. D **22**, 2157 (1980), *ibid.* **24**, 1808 (1981).
- [28] M. Diehl, Th. Feldmann, R. Jakob, and P. Kroll, Eur. Phys. J. C **8**, 409 (1999).
- [29] T. Shigetani, K. Suzuki, and H. Toki, Phys. Lett. B **308**, 383 (1993).
- [30] J. T. Lonergan, G. Q. Liu, and A. W. Thomas, Phys. Lett. B **380**, 393 (1996).
- [31] A. Edin and G. Ingelman, Phys. Lett. B **432**, 402 (1998).

## FIGURE CAPTIONS

Fig. 1.  $s(x) - \bar{s}(x)$  calculated in the MCM and LCM. The thin solid and thick solid curves are the contributions from  $\Lambda K$  component and  $\Lambda K$  plus  $\Sigma K$  components respectively, obtained in the MCM. The cut-off parameter in the form factor involved in the MCM has been taken as  $\Lambda = 1.08$  GeV. The thin dashed and thick dashed curves are the contributions from  $\Lambda K$  component and  $\Lambda K$  plus  $\Sigma K$  components respectively, obtained in the LCM with the parameter  $\alpha = 0.33$  GeV.

Fig. 2.  $s(x) - \bar{s}(x)$  calculated in the MCM with both  $\Lambda K$  and  $\Sigma K$  components included. The dotted, solid, and dashed curves are the results with cut-off parameters  $\Lambda = 1.00$  GeV, 1.08 GeV, and 1.20 GeV respectively.

Fig. 3.  $s(x) - \bar{s}(x)$  calculated in the MCM and LCM with both  $\Lambda K$  and  $\Sigma K$  components included. The solid curve is the result from the MCM with  $\Lambda = 1.08$  GeV. The dotted, dashed, and dashed-dotted curves are the predictions from the LCM with  $\alpha = 0.33$  GeV, 0.50 GeV and 1.00 GeV respectively.

Fig. 4.  $s$  and  $\bar{s}$  distributions in the baryon  $\Lambda$  ( $\Sigma$ ) and the meson  $K$ . The solid curve is the parametrization of GRV98 for  $s^B$ . The thin dotted and thick dotted curves are the  $s^B$  employed in the LCM with  $\alpha = 0.33$  GeV and 1.00 GeV respectively. The dashed-dotted curve is the parametrization of GRS98 for  $\bar{s}^K$ . The thin dashed and thick dashed curves are the  $\bar{s}^K$  employed in the LCM with  $\alpha = 0.33$  GeV and 1.00 GeV respectively.

Fig. 5. Fluctuation functions for  $N \rightarrow \Lambda K$  with the probability being 1.27%. The solid curve is the result from MCM with  $\Lambda = 1.08$  GeV. The dotted, dashed, and dashed-dotted curves are the results from LCM with  $\alpha = 0.33$  GeV, 0.50 GeV, and 1.00 GeV respectively.

Fig. 6. Fluctuation functions for  $N \rightarrow \Lambda K$  calculated in the MCM. The dotted, solid, and dashed curves are obtained with  $\Lambda = 1.00$  GeV, 1.08 GeV, and 1.20 GeV respectively, which corresponds to  $P_{\Lambda K} = 0.83\%$ , 1.27%, 2.42% respectively.

Fig. 7.  $s(x) - \bar{s}(x)$  calculated in the MCM and MLCM with both  $\Lambda K$  and  $\Sigma K$  components included. The solid curve is calculated in the MCM with  $\Lambda = 1.08$  GeV. The dotted, dashed, and dashed-dotted curves are the results from MLCM with  $\alpha = 0.33$  GeV, 0.50 GeV, and 1.00 GeV, respectively.

Fig. 1.

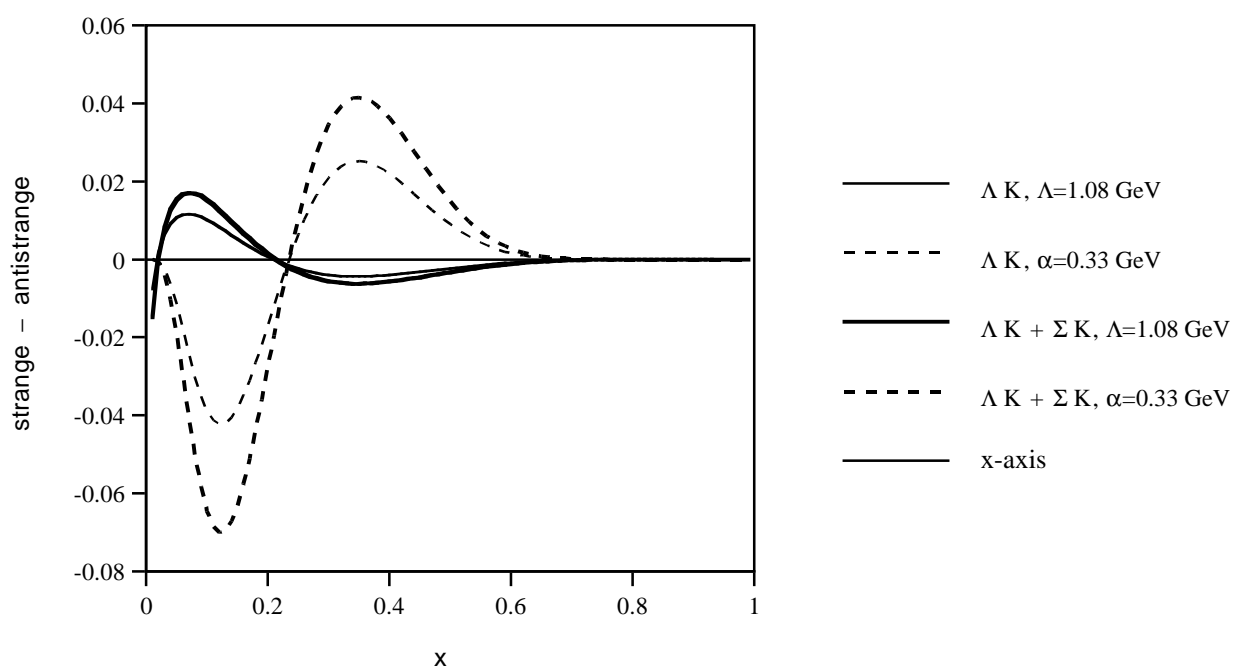


Fig. 2.

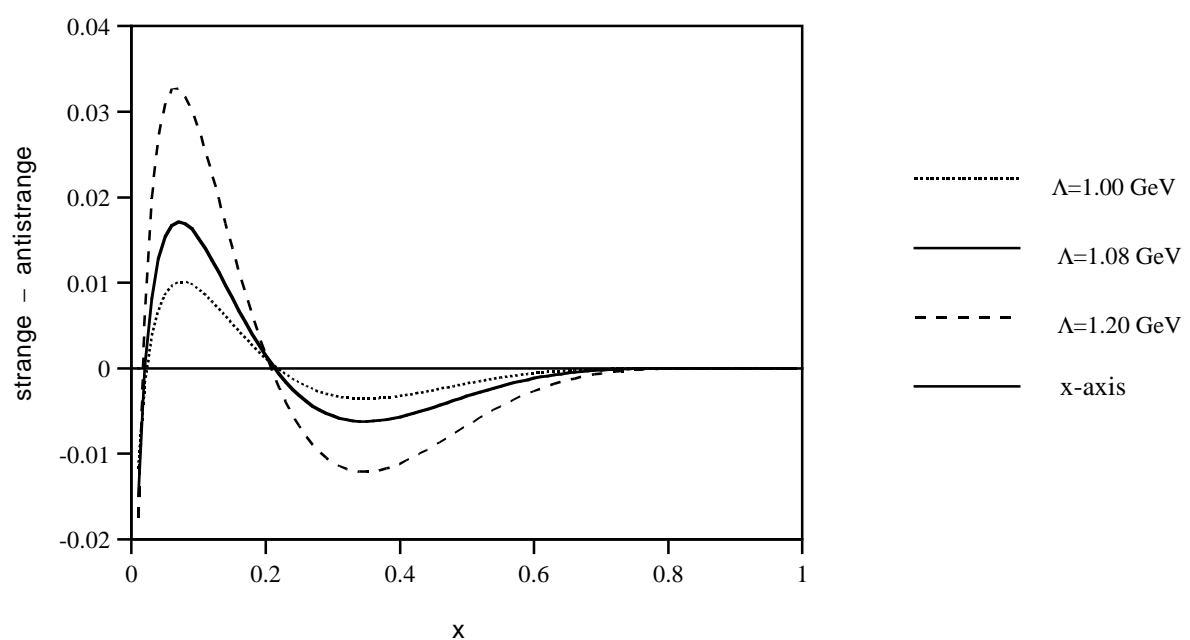


Fig. 3.

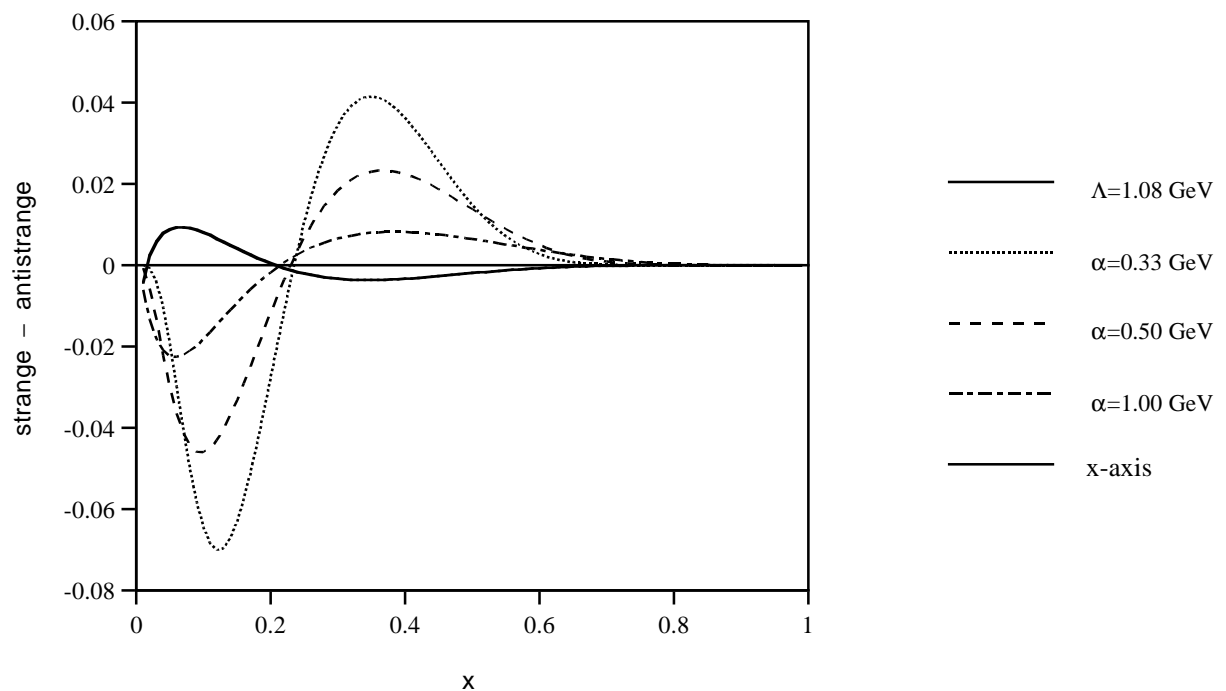


Fig. 4.

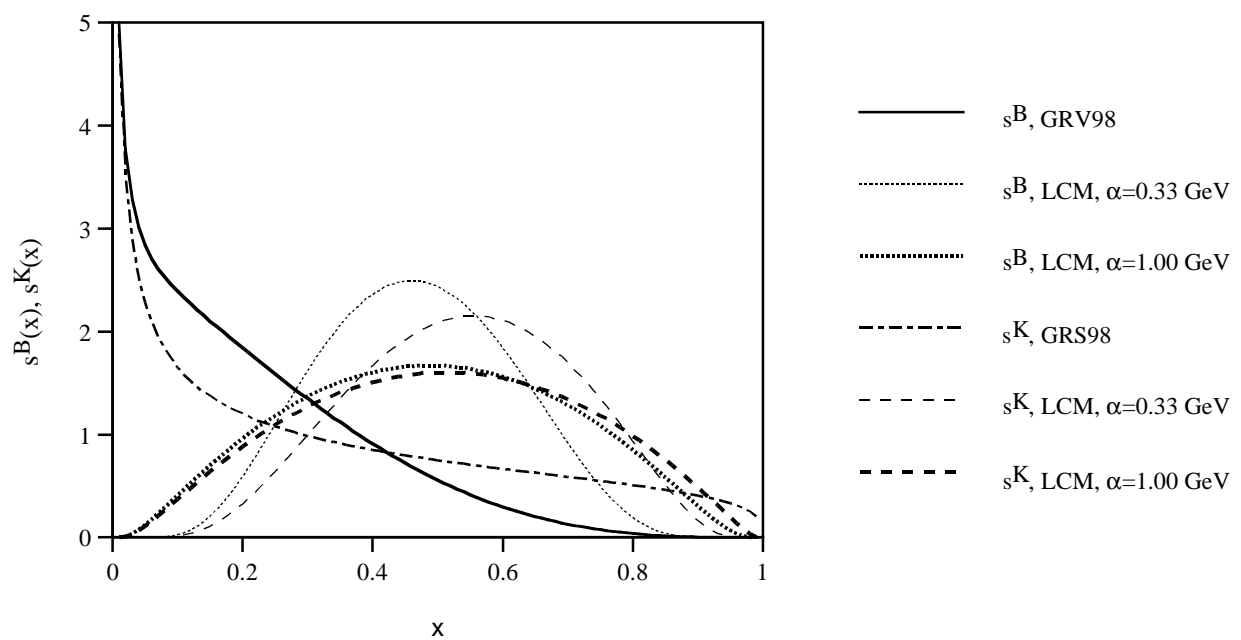


Fig. 5.

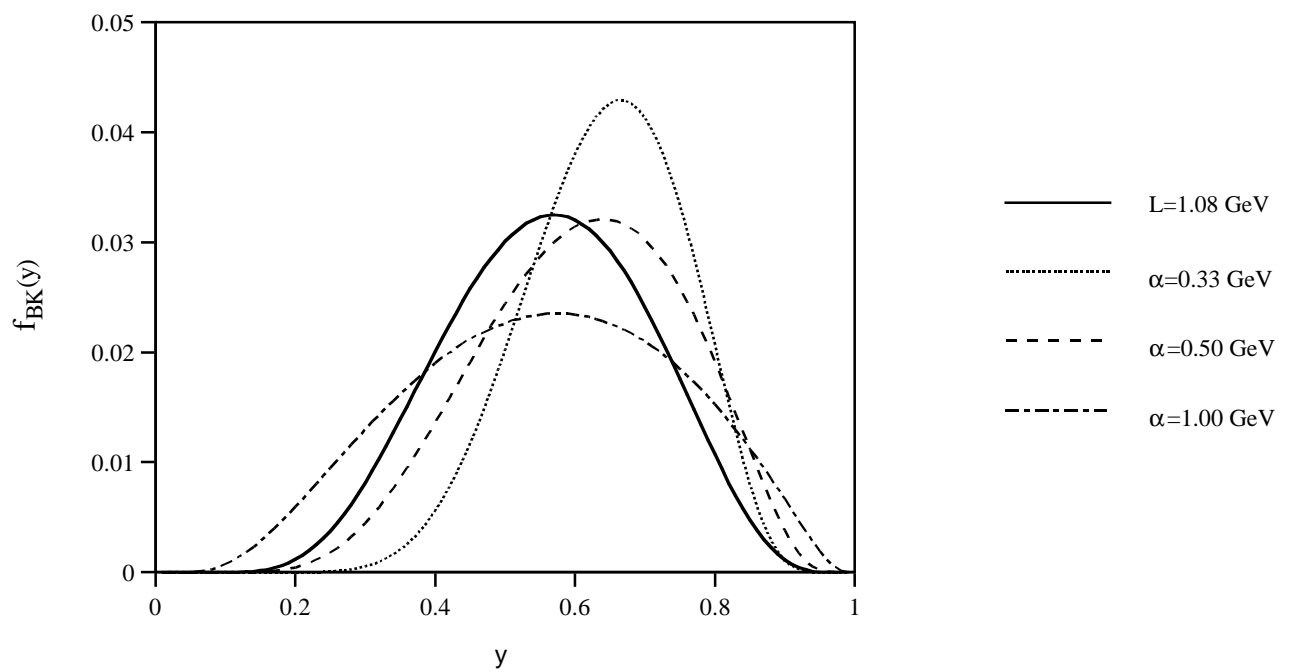


Fig. 6.

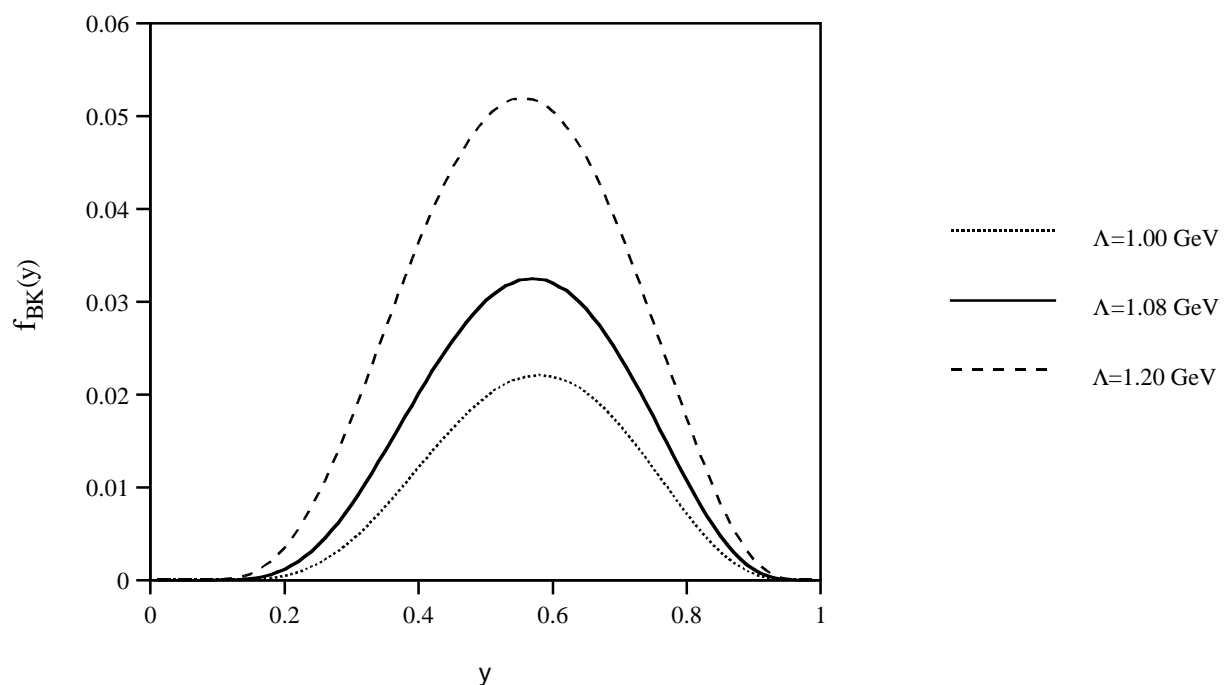


Fig. 7.

